Two-dimensional exciton dynamics and gain formation processes in $In_xGa_{1-x}N$ multiple quantum wells

Akihiro Satake and Yasuaki Masumoto
Institute of Physics, University of Tsukuba, Tsukuba, Ibaraki 305-8571, Japan
and Single Quantum Dot Project, ERATO, JST, Tsukuba, Ibaraki 300-2635, Japan

Takao Miyajima, Tsunenori Asatsuma, and Masao Ikeda
Research Center, Sony Corporation, Yokohama, Kanagawa 240-0031, Japan
(Received 26 May 1999)

We investigated exciton dynamics in $In_xGa_{1-x}N$ multiple quantum wells at 2 K and room temperature by means of time-resolved photoluminescence and pump-and-probe measurements. Under low excitation density, the temporal change of the spontaneous emission indicated slow dynamical features of the two-dimensional exciton localization, while, above a stimulation threshold density, the decay time of the emission was shortened to be less than ~30 ps due to the stimulated emission process. Further, the time-resolved pump-and-probe measurement revealed a fast relaxation of photoexcited delocalized electron-hole (e-h) pairs into localized states. Above stimulation threshold, localized states were saturated, and e-h pairs at delocalized states were observed. Two-dimensional e-h pairs at delocalized states relaxed into localized states and excitons were formed, from which the optical gain was formed in terms of the stimulated emission process.
[S0163-1829(99)13047-9]

I. INTRODUCTION

$In_xGa_{1-x}N$ ternary alloys are attracting much interest because of their applications as light-emitting devices in the green, blue, and UV energy regions. Blue/green single-quantum-well light-emitting diodes[1] and blue multiple-quantum-well laser diodes[2] contain the active layers of the $In_xGa_{1-x}N$ ternary alloys. Therefore, it is important to know the radiative recombination mechanism and the lasing mechanism in the $In_xGa_{1-x}N$ ternary alloys to make further progress in their applications. Recently, it has been reported that spontaneous emission from the $In_xGa_{1-x}N$ layers is related to the radiative recombination of excitons (carriers) localized at certain potential minima in the $In_xGa_{1-x}N$ layers.[3–10] Furthermore, it has been proposed that localized excitons (carriers)[3–10] or electron-hole (e-h) plasma[11] produce the stimulated emission process, but a definitive conclusion has not yet been obtained. It is important to make this problem clear.

The localization of carriers has been reported in many ternary alloy systems.[12–18] In mixed crystals, the disordered effect can be easily observed through a broadening of the optical spectra due to the formation of band-tail states. The density of states for the localized carriers has the form of an exponential tail extending down to the forbidden gap by a few tens of meV.[12,14,18] In the $In_xGa_{1-x}N$ ternary alloy system, there are several origins of the localized states in quantum wells: random well width variations, spatial compositional fluctuations, and complete phase separation. The potential inhomogeneities caused by such effects have been known. Transmission electron microscopy indicates the presence of an In-rich region acting as quantum dots,[7] and cathodoluminescence spectra mapping indicates that the In-rich area is smaller than 60 nm.[6] The localized states strongly influence the recombination properties and the processes of the carrier migration. In addition, optical gain can be observed due to the gradual filling of the localized states under moderate pumping.[18]

The dynamical optical properties of the $In_xGa_{1-x}N$ ternary alloy system have been reported by means of time-resolved luminescence measurements.[8–10] Most reports are about spontaneous emission, and there have been few reports about the stimulated emission. The lifetime of the spontaneous emission from the $In_xGa_{1-x}N$ ternary alloy system ranges from hundreds of picoseconds to a few nanoseconds, while that of the stimulated emission is less than tens of picoseconds.[9,10] This fact indicates that the stimulated emission process is completed within tens of picoseconds.

Reports about the optical gain spectra have been presented by means of the variable excitation-stripe length method[11,19,20] and the nanosecond nondegenerate optical pump-and-probe experiments.[21] In these methods, a dynamic phenomenon cannot be observed although a static phenomenon can be observed. Because the stimulated emission process in the $In_xGa_{1-x}N$ ternary alloys is completed within tens of picoseconds, it is very important to know the dynamical gain processes. Time-resolved pump-and-probe method provides direct information on the photoexcited carrier dynamics in semiconductor materials, because it can observe the distribution of the photoexcited carriers.[22] Hence this method is important for an investigation of the gain formation dynamics and the stimulation mechanism.

In this paper, we study the stimulated emission in optically pumped $In_xGa_{1-x}N$ multiple quantum wells (MQW's) at 2 K and room temperature (RT). We have also investigated the exciton dynamics of the $In_xGa_{1-x}N$ MQW's by means of a time-resolved photoluminescence (PL) measurement and a time-resolved pump-and-probe measurement employing white-light pulses in the picosecond and femtosecond time domains, respectively.

II. EXPERIMENTAL PROCEDURE

The sample used in our study was grown on a (0001)-oriented sapphire substrate by metal-organic chemical vapor deposition. The sample consisted of a GaN buffer layer, an undoped GaN layer 1.5 μm thick, a Si-doped GaN layer 20 nm thick, an active layer of Si-doped $In_xGa_{1-x}N$ MQW's, and a Si-doped GaN layer 80 nm thick. The active layer was 25 alternative periods of a 2-nm-thick $In_{0.11}Ga_{0.89}N$ quantum well and a 4-nm-thick $In_{0.03}Ga_{0.97}N$ barrier layer. The sample was evaluated in both the average indium concentration of the MQW's and the period of the MQW's by means of a x-ray-diffraction measurement. The diffraction lines of GaN(0004), $In_xGa_{1-x}N$, and its satellite peaks were obtained by the θ-2θ scan. We estimated the average indium concentration to be $x=0.057$ from the peak position of the $In_xGa_{1-x}N$ line, by taking account of the strain in the same way that was used in Ref. 23. The spectrum clearly showed higher-order satellite peaks, indicating the high interface quality and uniformity of the thickness.

Time-resolved PL measurement was performed by use of a synchroscan streak camera connected to a 25-cm-subtractive dispersion double monochromator. The time resolution was about 30 ps. The laser source was a self-mode-locked Ti:sapphire laser and a Ti:sapphire regenerative amplifier. The amplified output pulses had the pulse duration of 300 fs and a repetition rate of 200 kHz. The second harmonics of the amplified laser pulses was used as the excitation source. For a time-resolved pump-and-probe measurement employing white-light pulses, the laser source was a Ti:sapphire regenerative amplifier whose output pulses had a pulse duration of 300 fs and a repetition rate of 1 kHz. The second harmonics of the amplified laser pulses was used as the pump beam. A part of the amplified laser pulses was focused in pure water to produce white-light pulses, which were used as the probe beam. The transient absorption spectra were recorded by a 25-cm spectrometer and a liquid-nitrogen-cooled charge-coupled device multichannel detector.

III. RESULTS AND DISCUSSION

Figures 1(a) and 1(b) show the absorption spectrum and PL spectra at 2 K and RT, respectively. In mixed crystals, the density of the tail states is considered to be an exponential shape.[12–18] We can observe lower-energy tail states at the absorption spectrum in this sample. The areal density of the tail states $D(E)$ is well fitted by

$$D(E)=A\exp\left(\frac{E-E_{me}}{\epsilon}\right), \tag{3.1}$$

where ϵ is the characteristic energy indicating the broadening of the tail states, and E_{me} is the mobility edge. The fitting parameters are $\epsilon=84$ meV, $A=1.87\times10^{13}$ eV^{-1} cm^{-2}, and $E_{me}=3.178$ eV at 2 K; and $\epsilon=91$ meV, $A=1.70\times10^{13}$ eV^{-1} cm^{-2}, and $E_{me}=3.121$ eV at RT, respectively. The mobility edge is obtained from the kink point in the PL photon energy–excitation photon energy chart in the same manner that was used in our previous works.[9,10] In the absorption spectrum, we cannot see the exciton absorption. The reason for this is that the localization energy is so large

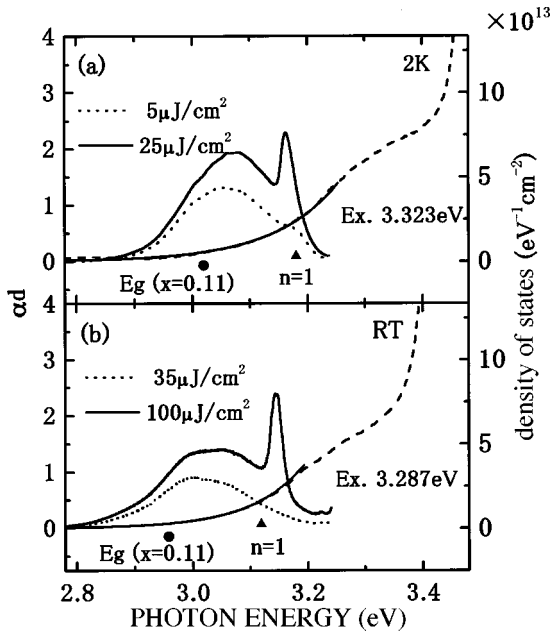

FIG. 1. (a) Absorption spectrum (dashed line) and time-integrated PL spectra of $In_xGa_{1-x}N$ MQW's at 2 K. The excitation energy densities are 5 (dotted line) and 25 μJ/cm^2 (solid line), respectively. The absorption tail is fitted by Eq. (3.1) in the text. The closed circle and the triangle show the band gap of the $In_{0.11}Ga_{0.89}N$ ternary alloy E_g and the lowest energy transition $n=1$ in the $In_{0.11}Ga_{0.89}N$ (2 nm)/$In_{0.03}Ga_{0.97}N$ (4 nm) MQW's obtained by the calculation, respectively. (b) Absorption spectrum (dashed line) and time-integrated PL spectra at RT. The excitation energy densities are 35 (dotted line) and 100 μJ/cm^2 (solid line), respectively.

that the exciton absorption becomes broad and is hidden under the tail of the continuous states.

The band gap of $In_xGa_{1-x}N$ ternary alloy is given by

$$E_{InGaN}(x)=(1-x)E_{GaN}+xE_{InN}-bx(1-x), \tag{3.2}$$

where b is known as a bowing parameter. The bowing parameter has a large value of $b=3.2$ eV for the $In_xGa_{1-x}N$ ternary alloy, with $x<0.2$.[23] The band gaps of the $In_{0.11}Ga_{0.89}N$ ternary alloy at 2 K and RT are obtained from Eq. (3.2) to be 3.02 and 2.96 eV, respectively. In the two-dimensional system, the transition energy between quantum levels in $In_xGa_{1-x}N$ quantum wells should be shifted to higher energy from the band gap due to confinement effects. We estimate the lowest quantized energy transition ($n=1$) in $In_{0.11}Ga_{0.89}N$ (2 nm)/$In_{0.03}Ga_{0.97}N$ (4 nm) MQW's by use of the finite potential well model. The lowest quantized energy transition ($n=1$) at 2 K and that at RT are estimated to be about 3.18 and 3.12 eV, respectively. In this calculation, a band-offset ratio of 4:1 for the conduction and valence bands is assumed.[24] The effective electron and hole masses of the $In_{0.11}Ga_{0.89}N$ quantum wells are $0.19m_0$ and $0.77m_0$, respectively, which are estimated by liner extrapolation of the effective masses in GaN, $0.2m_0$ and $0.8m_0$,[25,26] and InN, $0.12m_0$ and $0.5m_0$,[27] respectively. Because the calculated band gap of $In_{0.11}Ga_{0.89}N$ is lower than the mobility edge, and the calculated lowest quantized energy transition is very close to the mobility edge, two-dimensional confinement effects are considered to be present in this sample.

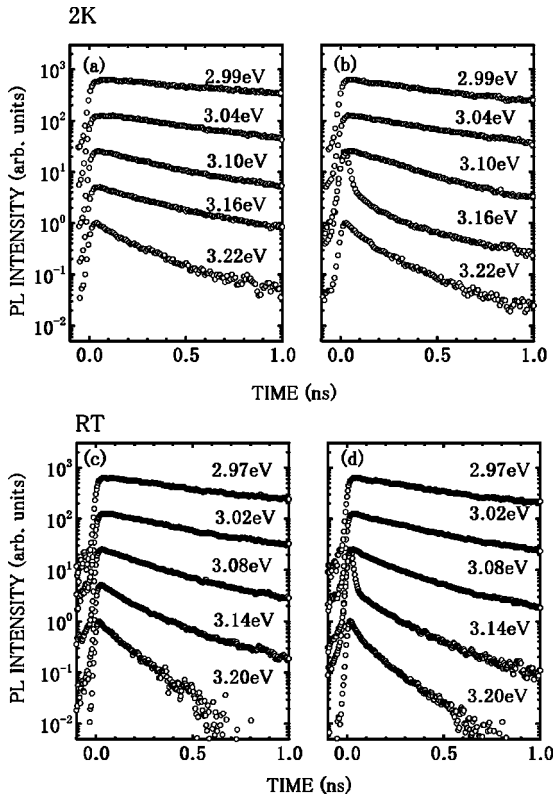

FIG. 2. Time-resolved PL at 2 K obtained under excitation energy densities of (a) 5 and (b) 25 μJ/cm^2, respectively. The detection photon energies are 2.99, 3.04, 3.10, 3.16, and 3.22 eV. The decay of the stimulated emission is observed at 3.16 eV in (b). Time-resolved PL at RT obtained under excitation energy densities of (c) 35 and (d) 100 μJ/cm^2, respectively. The detection photon energies are 2.97, 3.02, 3.08, 3.14, and 3.20 eV. The decay of the stimulated emission is observed at 3.14 eV in (d).

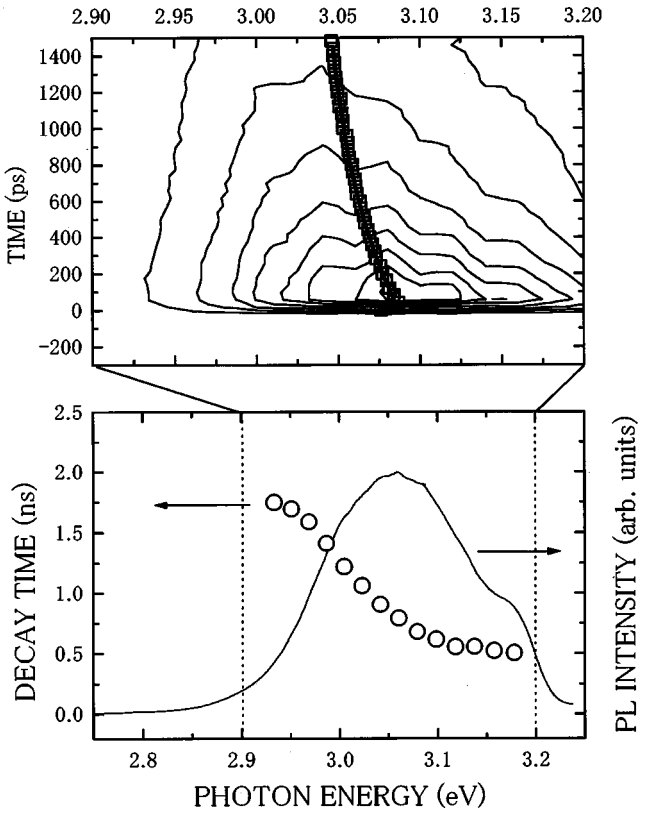

FIG. 3. (a) A contour map of the energy- and time-resolved PL intensity at 2 K. The excitation photon energy is 3.323 eV. Open squares show the PL center of the gravity as a function of time. (b) Time-integrated PL spectrum. Open circles show the decay time observed at various photon energies.

The time-integrated PL spectra at 2 K under excitation energy densities of 5 (dotted line) and 25 μJ/cm^2 (solid line) are shown in Fig. 1(a). The excitation photon energy is 3.323 eV, which is lower than the band gap of GaN layer. In this condition, we can discuss the exciton dynamics only in the active layer of the $In_xGa_{1-x}N$ MQW's. Under an excitation energy density of 5 μJ/cm^2, the PL spectrum has a broad spontaneous emission band with a full width at half maximum (FWHM) of about 185 meV. The peak position of the spontaneous emission is located at 3.06 eV, which shows a Stokes shift from the absorption band. The decay time of the spontaneous emission shows a nearly single-exponential decay, and the decay time increases with a decrease of the detection photon energy, as shown in Fig. 2(a). The decay times of the various observed photon energies are shown with the time-integrated PL spectrum in Fig. 3(b). Under an excitation energy density of 25 μJ/cm^2, we can observe a sharp stimulated emission band at the higher-energy side of the spontaneous emission. The peak position of the stimulated emission is located at 3.16 eV, and the FWHM is about 20 meV. The stimulation threshold is 17 μJ/cm^2 obtained from the excitation intensity dependence of the PL intensity. The decay time of the stimulated emission is less than $\sim$30 ps, as shown in Fig. 2(b). The temporal trace at 3.16 eV indicates a transformation from the stimulated emission to the spontaneous one.

The time-integrated PL spectra at RT are shown in Fig. 1(b). The excited photon energy is 3.287 eV. The excitation energy densities are 35 (dotted line) and 100 μJ/cm^2 (solid line), respectively. The peak position of the spontaneous emission is located at 3.01 eV with a FWHM of about 185 meV. Above the stimulation threshold, we can observe stimulated emission even at RT. The peak position of the stimulated emission is located at 3.14 eV. The temporal traces of the PL at RT are shown in Figs. 2(c) and 2(d). The decay of the spontaneous emission shows a nearly single-exponential decay, and the decay time increases with the decrease of the detection photon energy, similar to what happens at 2 K. The decay time of the stimulated emission is less than $\sim$30 ps, similar to what happens at 2 K. The experimental features at RT are so similar to those at 2 K that the physical mechanisms of the emission at 2 K and RT are considered to be the same. Because the experimental results at 2 K are clear than those at RT, we mainly discuss the results at 2 K in the following.

We discuss the slow energy relaxation under low excitation density. Figure 3(a) shows the energy- and time-resolved PL at 2 K under an excitation energy density of 5 μJ/cm^2. This figure is constructed from a spectrally resolved temporal change of the PL. The open squares in Fig. 3(a) indicate the temporal change of the center of gravity of the spontaneous emission, which is defined by

$$\langle E(t)\rangle = \left(\sum_i E_i f(E_i,t)\right) \Big/ \left(\sum_i f(E_i,t)\right), \quad (3.3)$$

where $f(E_i,t)$ is the spectrally resolved temporal change of the spontaneous emission, and E_i corresponds to the observed photon energy. As time passes, the center of gravity of the spontaneous emission shifts toward lower photon energy. It is well fitted by

$$\langle E(t)\rangle = 3.037 + 0.05 \times \exp\left(-\frac{t}{896\ \text{ps}}\right)\ (\text{eV}), \quad (3.4)$$

and the decrease rate of the photon energy is 3×10^7 eV/s, as shown by the solid line in Fig. 3(a). There can be a kinetic-energy loss process for the energy relaxation of the carriers. In this process, the carriers are scattered to smaller **k** states as the result of the phonon emission. The kinetic-energy loss rate of the two-dimensional carriers via deformation-potential-type interaction with the acoustic phonons is calculated by[28,29]

$$\left\langle \frac{dE(t)}{dt} \right\rangle = \frac{2M^2D^2}{\hbar^3\rho}[k_B T_e(t) - k_B T_L]. \quad (3.5)$$

Here M is the carrier mass, D is the deformation potential, ρ is the areal mass density, $T_e(t)$ is the effective temperature of the two-dimensional carriers, and T_L is the lattice temperature. By using the values for GaN, $m_e=0.2m_0$, $m_h=0.8m_0$, $D_e=59.9$ eV, $D_h=44.5$ eV, $D_{ex}=D_e-D_h=15.4$ eV,[30,31] and $\rho=\rho_{3D}L_z=(6.11\ \text{g/cm}^3)\times(2\ \text{nm})$,[32] the relaxation time constant of the two-dimensional electrons (holes) is estimated to be 2.3 ps (0.27 ps), and that of the two-dimensional excitons to be 55 ps, which are much faster than the observed one. The observed slow energy-loss rate is interpreted by the energy relaxation model for the two-dimensional exciton localization.[33,34]

The relaxation processes of the localized excitons are explained as follows. Photogenerated two-dimensional *e-h* pairs at delocalized states have a kinetic energy far exceeding the amplitude of the potential fluctuations. The *e-h* pairs have a high probability of spatial migration, and lose their energy quickly via acoustic-phonon interaction. After most of the kinetic energy is lost, electrons or holes are captured at localized states and exitons are formed, where the energy-loss processes are mainly due to spatial migration between the localized states with the emission of acoustic phonons. The relaxation rate of such processes depends strongly on the density of the available final states at the lower energy. The decay rate of the localized states is expressed by the relaxation rate to lower-energy states minus that to localized states from higher-energy states, plus the radiative recombination rate. Therefore, the decay time increases with the decrease of the detection photon energy, and the center of gravity of the spontaneous emission shifts toward a lower photon energy as time passes.

Under high excitation density, we can observe stimulated emission at the higher energy side of the spontaneous emission. The stimulation threshold is 17 μJ/cm^2 at 2 K. We consider that the stimulated emission can be attributed to localized excitons because the stimulated emission is just below the mobility edge. The optical gain for the mixed crystals is due simply to the filling of the localized states, and the gain peak is observed at the highest density.[18] The carrier areal density at the stimulation threshold (17 μJ/cm^2) is estimated to be $n=2.5\times10^{12}$ cm^{-2} at the first layer in the

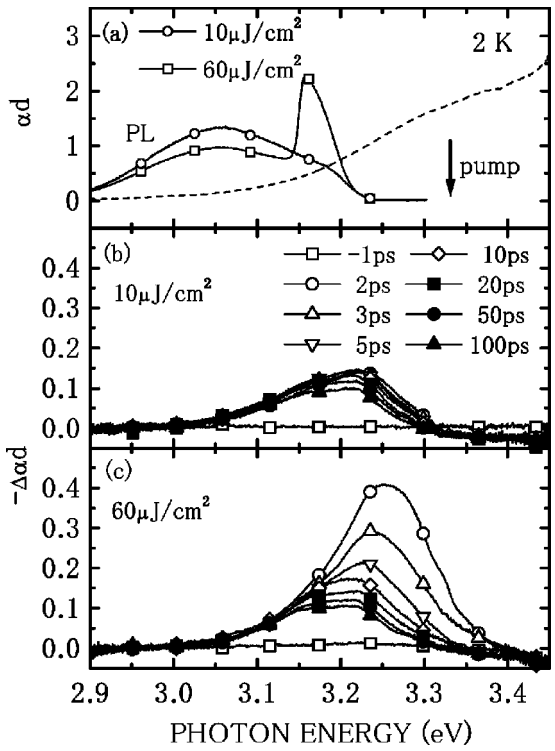

FIG. 4. The pump-and-probe measurement at 2 K. (a) The dashed line shows the absorption spectrum without pumping. The solid lines show the PL spectra under excitation densities of 10 (open circles) and 60 μJ/cm^2 (open squares), respectively. The excitation photon energy is 3.323 eV. The time-resolved differential absorption spectra under excitation energy densities of (b) 10 and (c) 60 μJ/cm^2, respectively.

$In_xGa_{1-x}N$ MQW's ($n=1.1\times10^{12}$ cm^{-2} is the average areal density). This value is below the density necessary for the formation of an *e-h* plasma, which is given in the first approximation by $n_p=1/\pi(a_B^{2D})^2=9.8\times10^{12}$ cm^{-2} for the parameters in GaN, where $a_B^{2D}=1.8$ nm is the two-dimensional (2D) Bohr radius of the exciton estimated by the theoritical value of $a_B^{3D}/2$. In addition, it has been known that the many-body effects are reduced as long as the carriers are localized in mixed crystals.[35] Under quasi-steady-state condition, the delocalized states are occupied only when the total density of the *e-h* pairs exceeds the density of the localized states under strong excitation. The total areal density of the localized states is estimated to be an order of 10^{12} cm^{-2} in the sample from the absorption spectrum. This means that the localized states are able to accommodate all carriers produced by the excitation. Therefore, the possibility of *e-h* plasma formation can be ruled out in the stimulation mechanism in the $In_xGa_{1-x}N$ MQW's.

The stimulated emission process was found to be fast within tens of picoseconds from a time-resolved PL measurement. To directly the exciton relaxation observe, and discuss the gain formation processes, we performed a time-resolved pump-and-probe measurement employing white-light pulses. Figure 4(a) shows the absorption spectrum (dashed line) without pumping and the PL spectra (solid lines) at 2 K under excitation energy densities of 10 (open circles) and 60 μJ/cm^2 (open squares), respectively. The excitation photon energy is 3.323 eV. Figures 4(b) and 4(c) show the temporal changes of the differential absorption

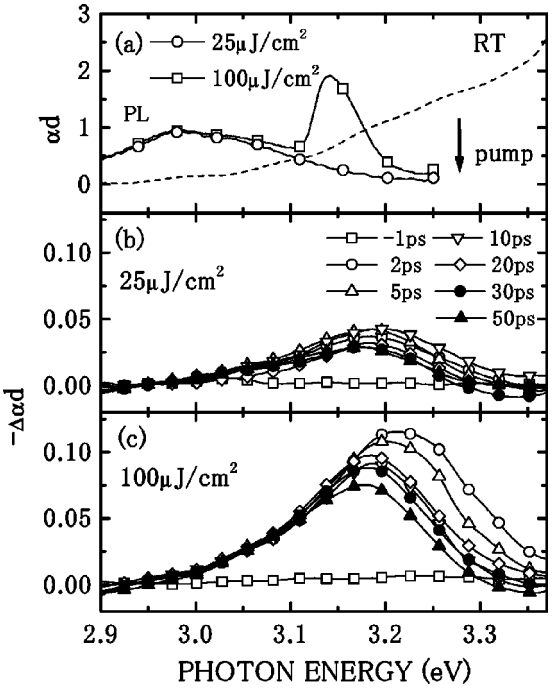

FIG. 5. The pump-and-probe measurement at RT. (a) The dashed line shows the absorption spectrum. The solid lines show the PL spectra under excitation densities of 25 (open circles) and 100 μJ/cm^2 (open squares), respectively. The excitation photon energy is 3.278 eV. The time-resolved differential absorption spectra under excitation energy densities of (b) 25 and (c) 100 μJ/cm^2, respectively.

spectra under excitation energy densities of 10 and 60 μJ/cm^2, respectively. The upward vertical direction means a bleaching of the absorption. Under both excitation energy densities, the differential absorption spectra show negative signals at the lower-energy tail states (localized states), and the signals are almost proportional to the state density below a photon energy of 3.16 eV. The signal hardly changes within 100 ps because relaxation at the localized states is very slow. Under an excitation energy density of 10 μJ/cm^2, a positive signal, that is the induced absorption, is clearly observed above a photon energy of 3.3 eV. On the other hand, above the stimulation threshold, the signals at the higher-energy states (delocalized states) have drastic changes within 20 ps. After 20 ps, the signals are comparable to signals below the stimulation threshold. Comparing the temporal change of the differential absorption with that of the PL, we note that the rapid decay observed as the stimulated emission by the time-resolved PL measurement is not repeated at the same position by the time-resolved pump-and-probe measurement. This phenomenon indicates that the localized states are saturated, and that many *e-h* pairs are in the delocalized states. Optical gain is possible due to the localized states, and *e-h* pairs are supplied to localized states from delocalzed states and the excitons are formed.

Similar results are obtained at RT. Figure 5(a) shows the absorption spectrum (dashed line) and the PL spectra (solid lines) at RT under excitation energy densities of 25 (open circles) and 100 μJ/cm^2 (open squares), respectively. The excitation photon energy is 3.278 eV. The differential absorption spectra are shown in Figs. 5(b) and 5(c). Below the stimulation threshold, the negative signals hardly change. Above the stimulation threshold, drastic changes are observed at the delocalized states within 20 ps. This behavior of the signals at RT is similar to that of the signals at 2 K. Therefore, we can conclude from the results that the optical gain is formed by the same mechanism at 2 K and RT.

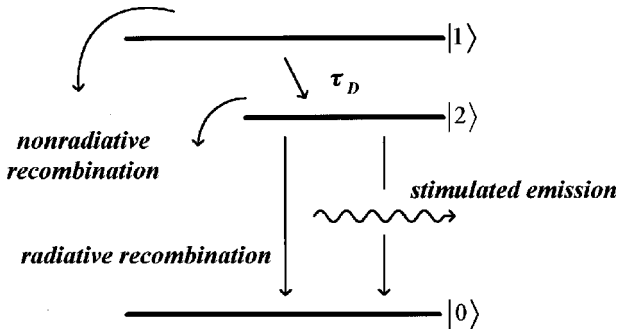

FIG. 6. Schematic illustration of the relaxation model.

We explain the fast energy relaxation concerned with the stimulation process by use of a simplified three-energy-level scheme, as shown in Fig. 6. Now we consider a delocalized site, a localized site and the ground state. Actually, the delocalized and localized sites cause the energy distribution, and form the bands, respectively. The photogenerated *e-h* pairs diffuse and relax rapidly into the delocalized site, and then relax into the localized site, and then excitons are formed. Since the filling of the localized site prevents relaxation from the delocalized site to the localized site, the relaxation rate depends on the occupation probability of the localized site. As a result of a filling of the localized states, optical gain is possible from the localized site due to the stimulated emission process, and some excitons emit photons as the lasing mode. Some excitons recombine radiatively or nonradiatively, including the spatial migration mode between the localized states. Then the rate equations in this model are given by

$$\frac{dN_1}{dt} = -\frac{N_1}{\tau_{r1}} - \frac{N_1}{\tau_D}, \tag{3.6}$$

$$\frac{dN_2}{dt} = \frac{N_1}{\tau_D} - \frac{N_2}{\tau_{r2}} - \alpha S. \tag{3.7}$$

Here N_1 is the number of *e-h* pair at the delocalized site, N_2 is that of excitons at the localized site, and S is given by $S = N_2 - N_{th}$, where N_{th} is the threshold number of the excitons. τ_{r1}^{-1} is the recombination rate at the delocalized site, τ_{r2}^{-1} is that at the localized site, α is that via the stimulation mode, and τ_D^{-1} is the relaxation rate derived from the delocalized site to the localized site given by $\tau_D^{-1} = \tau_0^{-1}(1 - N_2/N_{2max})$, where N_{2max} is the maximum number of the excitons in the localized site and τ_0^{-1} is the relaxation rate in the unoccupied localized state. Now we consider the condition $\tau_{r2}^{-1} < \tau_{r1}^{-1} \ll \tau_0^{-1} < \alpha$. In this condition, the temporal change of the *e-h* pair at the delocalized site has a rapid decay time τ_D, and that at the localized site has a rapid rise time τ_D, and a slow radiative decay time τ_{r2} is assumed below the stimulation threshold. Above the stimulation threshold, the temporal change of the excitons at the local-

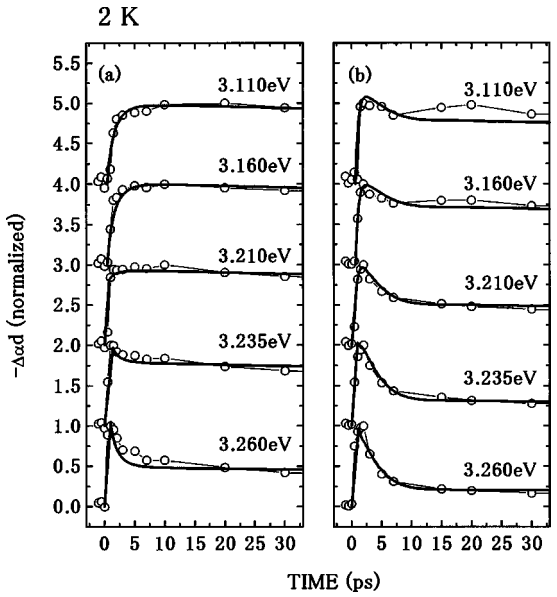

FIG. 7. Temporal changes of the differential absorption obtained under excitation energy densities of (a) 10 and (b) 60 μJ/cm^2 at 2 K. Bold solid lines are calculated by the three-energy level scheme.

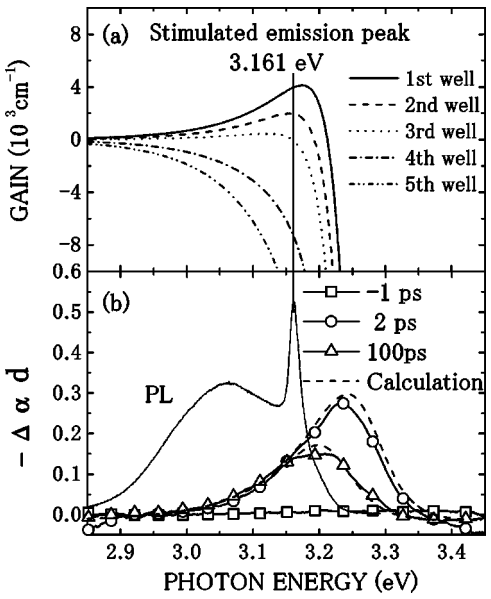

FIG. 8. (a) The calculated gain spectra at each quantum well in the MQW's under an excitation energy density of 20 μJ/cm^2 at 2 ps. These are calculated by taking account of the depth profile of the carrier density. (b) The differential absorption spectra under an excitation energy density of 20 μJ/cm^2 with the time-integrated PL spectrum at 2 K. Solid lines show the differential absorption spectra at 2 (open circles) and 100 ps (open triangles). The dashed lines show the reproduced differential absorption spectra.

ized site has a rapid decay and a slow decay. Figure 7 shows calculations of the temporal changes of the number of excitons by use of the parameters $\tau_{r1}=100$ ps, $\tau_{r2}=500$ ps, $\tau_0=1$ ps and $\alpha^{-1}=1$ ps. The calculations explain the temporal changes of the excitons well, adjusting the ratio of the delocalized states and the localized states at the different photon energies. Thus optical gain is possible from the localized states as a result of a filling of the localized states. The *e*-*h* pairs are supplied to the localized states from the delocalized states.

Now the optical gain spectra for the $In_xGa_{1-x}N$ MQW's are analyzed by use of a phenomenological model for the inhomogeneously broadened system, which is proposed in II-VI compound semiconductors.[36] The excitons are localized due to the alloy compositional fluctuation and random well width variations, which leads to an inhomogeneously broadened absorption profile. The population inversion condition is decided on the occupancy probability of the localized site. If the localized site is occupied, the contribution is positive (gain). On the other hand, if it is unoccupied, the contribution is negative (absorption). In the simplified three-energy-level model, exciton relaxation occurs from the initial higher-energy states (delocalized states) to the lower-energy states (localized states), from which optical gain is possible due to stimulated emission to the ground state. In the extreme inhomogeneous broadening system, the gain/absorption coefficient can be written as

$$g(E)=D_i(E)[2f(E)-1], \tag{3.8}$$

where $D_i(E)$ is the inhomogeneous line-shape function and $f(E)$ is the energy distribution function. If all the states are empty, the absorption profile is obtained as $-D_i(E)$. The calculated gain spectra for the $In_xGa_{1-x}N$ MQW's at 2 ps under an excitation energy density of 20 μJ/cm^2 are shown in Fig. 8(a), in which we took account of the depth profile of the carrier density obtained by the absorption coefficient and the structure of the sample. We assumed the energy distribution function to be

$$f(E)=\frac{a}{\exp\left(\dfrac{E-b}{\epsilon}\right)+1}. \tag{3.9}$$

Here a, b, and ϵ are the calculation parameters, which are chosen so as to reproduce the differential absorption spectra. The reproduced differential absorption spectra at 2 and 100 ps are shown in Fig. 8(b). The energy position of the maximum gain obtained by the calculation agrees with the stimulated emission peak observed by the experiment. Thus the phenomenological model for the inhomogeneously broadened system explains the optical gain formation processes.

In the differential absorption spectra, we observed an induced absorption. One explanation for the induced absorption might be the existence of midgap states such as a trap state.[37,38] In this case, induced absorption can be observed over a wide range of photon energy, but it is inconspicuous due to the large contribution of the band-filling effect. Another explanation may be the redshift of the absorption spectrum. The induced absorption measured at 3.35 eV is $\Delta\alpha d=0.03$, which may correspond to a redshift of 5 meV of the absorption spectrum. We think that this absorption is not induced by the band-gap renormalization effect, because the induced absorption can be also observed in this sample under a low excitation density at 100 nJ/cm^2 by means of one-beam pump-and-probe measurement.[39] There is room for the argument concerning the course of the induced absorption, but it cannot be discussed here.

IV. CONCLUSIONS

In conclusion, we observed stimulated emission from optically pumped $In_xGa_{1-x}N$ MQW's at 2 K and RT, and investigated the exciton dynamics. The temporal changes of the spontaneous emission indicated the dynamical feature of the two-dimensional exciton localization. Time-resolved pump-and-probe measurement showed that photoexcited *e-h* pairs relaxed into localized states through delocalized states, and that excitons were formed in a few picoseconds. Over the stimulation threshold, the localized states were saturated, and many *e-h* pairs existed in the delocalized states within a few tens of picoseconds. This optical gain is possible in terms of the stimulated emission process from localized states, which causes fast relaxation from delocalized states to localized states. The stimulated emission was related to the filling of the localized states.

ACKNOWLEDGMENT

The authors wish to thank Dr. M. Ikezawa for technical support of the experiments.

[1] S. Nakamura, M. Senoh, N. Iwasa, S. Nagahama, T. Yamada, and T. Mukai, Jpn. J. Appl. Phys., Part 2 **34**, L1332 (1995).
[2] S. Nakamura, M. Senoh, S. Nagahama, N. Iwasa, T. Yamada, T. Matsushita, Y. Sugimoto, and H. Kiyoku, Appl. Phys. Lett. **70**, 1417 (1997).
[3] M. Smith, G.D. Chen, J.Y. Lin, H.X. Jiang, M. Asif Khan, and Q. Chen, Appl. Phys. Lett. **69**, 2837 (1996).
[4] S. Chichibu, T. Azuhata, T. Sota, and S. Nakamura, Appl. Phys. Lett. **69**, 4188 (1996).
[5] S. Chichibu, T. Azuhata, T. Sota, and S. Nakamura, Appl. Phys. Lett. **70**, 2822 (1997).
[6] S. Chichibu, T. Sota, and S. Nakamura, Appl. Phys. Lett. **71**, 2346 (1997).
[7] Y. Narukawa, Y. Kawakami, M. Funato, Sz. Fujita, Sg. Fujita, and S. Nakamura, Appl. Phys. Lett. **70**, 981 (1997).
[8] Y. Narukawa, Y. Kawakami, Sz. Fujita, Sg. Fujita, and S. Nakamura, Phys. Rev. B **55**, R1938 (1997).
[9] A. Satake, Y. Masumoto, T. Miyajima, T. Asatsuma, F. Nakamura, and M. Ikeda, Phys. Rev. B **57**, R2041 (1998).
[10] A. Satake, Y. Masumoto, T. Miyajima, T. Asatsuma, and M. Ikeda, J. Cryst. Growth **189-190**, 601 (1998).
[11] G. Mohs, T. Aoki, M. Nagai, R. Shimano, M. Kuwata-Gonokami, and S. Nakamura, Solid State Commun. **104**, 643 (1997).
[12] S. Permogorov, A. Reznitskii, S. Verbin, G.O. Müller, P. Flögel, and M. Nikiforova, Phys. Status Solidi B **113**, 589 (1982).
[13] S. Permogorov and A. Reznitsky, J. Lumin. **52**, 201 (1992).
[14] E. Cohen and M.D. Sturge, Phys. Rev. B **25**, 3828 (1982).
[15] M.D. Sturge, E. Cohen, and R.A. Logan, Phys. Rev. B **27**, 2362 (1983).
[16] A. Fried, A. Ron, and E. Cohen, Phys. Rev. B **39**, 5913 (1989).
[17] Y. Kawakami, M. Funato, Sz. Fujita, Sg. Fujita, Y. Yamada, and M. Masumoto, Phys. Rev. B **50**, 14 655 (1994).
[18] F.A. Majumder, S. Shevel, V.G. Lyssenko, H.E. Swoboda, and C. Klingshirn, Z. Phys. B: Condens. Matter **66**, 409 (1987).
[19] G. Frankowsky, F. Steuber, V. Härle, F. Scholz, and A. Hangleiter, Appl. Phys. Lett. **68**, 3746 (1996).
[20] Y.-K. Song, M. Kuball, A.V. Nurmikko, G.E. Bulman, K. Doverspike, S.T. Sheppard, T.W. Weeks, M. Leonard, H.S. Kong, H. Dieringer, and J. Edmond, Appl. Phys. Lett. **72**, 1418 (1998).
[21] T.J. Schmidt, Y.-H. Cho, G.H. Gainer, J.J. Song, S. Keller, U.K. Mishra, and S.P. DenBaars, Appl. Phys. Lett. **73**, 1892 (1998).
[22] F. Sasaki, T. Mishina, and Y. Masumoto, Phys. Rev. B **46**, 6750 (1992).
[23] T. Takeuchi, H. Takeuchi, S. Sota, H. Sakai, H. Amano, and I. Akasaki, Jpn. J. Appl. Phys., Part 2 **36**, L177 (1997).
[24] C.G. Van de Walle and J. Neugebauer, Appl. Phys. Lett. **70**, 2577 (1997).
[25] A.S. Barker and M. Ilegems, Phys. Rev. B **7**, 743 (1973).
[26] J.I. Pankove, S. Bloom, and G. Harbeke, RCA Rev. **36**, 163 (1975).
[27] C.P. Foley and T.L. Tansley, Phys. Rev. B **33**, 1430 (1986).
[28] Y. Masumoto, S. Shionoya, H. Kawaguchi, Phys. Rev. B **29**, 2324 (1984).
[29] K. Hess and C.T. Sah, Phys. Rev. B **10**, 3375 (1974).
[30] A. Shikanai, T. Azuhata, T. Sota, S. Chichibu, A. Kuramata, K. Horino, and S. Nakamura, J. Appl. Phys. **81**, 417 (1997).
[31] K. Shimada, T. Sota, and K. Suzuki, J. Appl. Phys. **84**, 4951 (1998).
[32] *Semiconductors, Physics of Group IV Elements and III-V Compounds*, edited by O. Madelung, Landolt Börnstein, New Series, Group III, Vol. 17, Pt. a (Springer-Verlag, Berlin, 1982).
[33] T. Takagahara, Phys. Rev. B **31**, 6552 (1985).
[34] Y. Masumoto, S. Shionoya, and H. Okamoto, in *Proceedings of the 17th International Conference on the Physics of Semiconductors, San Francisco, 1984*, edited by J. D. Chadi and W. A. Harrison (Springer-Verlag, New York, 1985), p. 349.
[35] C. F. Klingshirn, *Semiconductor Optics* (Springer, Berlin, 1995), Chap. 20, p. 306.
[36] J. Ding, H. Jeon, T. Ishihara, M. Hagerott, A.V. Nurmikko, H. Luo, N. Samarth, and J. Furdyna, Phys. Rev. Lett. **69**, 1707 (1992).
[37] Z. Vardeny, J. Strait, D. Pfost, J. Tauc, and B. Abeles, Phys. Rev. Lett. **48**, 1132 (1982).
[38] S.D. Benjamin, H.S. Loka, A. Othonos, and P.W.E. Smith, Appl. Phys. Lett. **68**, 2544 (1996).
[39] A. Satake, E. Tokunaga, Y. Masumoto, T. Miyajima, T. Asatsuma, and M. Ikeda (unpublished).